

CIRJE-F- 1197

**A State Space Modeling for Proactive Management  
in Equity Investment**

Akihiko Takahashi

The University of Tokyo

Soichiro Takahashi

GCI Asset Management, Inc.

July 2022

CIRJE Discussion Papers can be downloaded without charge from:  
<http://www.cirje.e.u-tokyo.ac.jp/research/03research02dp.html>

Discussion Papers are a series of manuscripts in their draft form. They are not intended for circulation or distribution except as indicated by the author. For that reason Discussion Papers may not be reproduced or distributed without the written consent of the author.

# A state space modeling for proactive management in equity investment\*

Akihiko Takahashi,

*Corresponding Author*

*Graduate School of Economics, University of Tokyo, 7-3-1 Hongo Bunkyo-ku, Tokyo, Japan, 113-0033*

Soichiro Takahashi

*GCI Asset Management, Inc., 9F Tokiwabashi Tower, 2-6-4 Otemachi, Chiyoda-ku, Tokyo, Japan, 100-0004*

July 20, 2022

## Abstract

This paper proposes a novel state-space approach to explain stock market dynamics driven by different types of trading, which leads to a new promising scheme for proactive risk management in financial investment. Particularly, it is assumed that the current price changes are formulated through daily trading by multiple types of traders, each of whom follows a specific investment strategy based on technical indicators and a fuzzy logic using past data of stock prices, volumes and yield curves. Moreover, the current price changes are represented by a linear combination of those multiple trading types, where the coefficients corresponding with the size of impact on the price changes are regarded as time-varying state variables to be sequentially estimated under a state-space framework. Thereby, this work develops a new factor decomposition method on price changes from a perspective of different traders' demand and supply to analyze the current situations and potential risks in financial markets.

In empirical experiments, it is shown that the implementation of particle filtering algorithm makes it possible to replicate market price changes. Further, new signals based on the estimated states are developed, which are applied to proactive risk management in financial investment. Especially, it has been found that the demands of yield curve-based traders subtracting those of trend-followers could be a promising signal of stock market crashes, which has successfully enhanced simple buy-and-hold strategy of SP, as well as constant proportion strategies.

**Keywords:** state-space model, fuzzy system, technical analysis, yield curve, trend following, proactive risk management

---

\*Forthcoming in *International Journal of Financial Engineering*

# 1 Introduction

Financial markets are well-known to be highly complex and non-linear systems with noise, which are affected by economic, political, geopolitical and psychological factors. Recently, for various financial market problems, artificial intelligence (AI) techniques have been increasingly used in both academia and industry, because they are effective to treat non-linearity or uncertainty. (Cavalcante et. al, 2016).

For instance, Nakano and Takahashi (2020) proposed a new approach to the portfolio management using an AutoEncoder, where factors obtained by an AutoEncoder are used to construct a downside hedged portfolio. Long et al.(2020) presented a framework fusing trading and market information for stock prediction, where the relevant stocks of the target stock are selected by knowledge graph methods. Yang et al.(2019) proposed a new stock scoring mechanism with a linear combination of the predicted factor based on computational intelligence and the fundamental factors. Zhou et al.(2019) developed a cascaded learning architecture to predict the direction of the daily changes of stock indices, combining logistic regression and gradient boosted decision trees. Ramezani et al. (2019) showed an integrated framework of genetic network programming and multi-layer neural network for prediction of daily stock return with an application in Tehran stock exchange market. Lei (2018) illustrated a Wavelet neural network-based trend prediction method of stock prices based on rough set attribute reduction. Dash et al.(2019) suggested a Crow search-based weighted voting classifier ensemble including TOPSIS for stock index movement prediction. Alimoradi and Kashan (2018) considered a league championship algorithm with network structure and backward Q-learning for extracting stock trading rules. Kristjanpoller and Michell (2018) attempted to improve well-known GARCH-based volatility forecasting using fuzzy neural network methods. Chang and Lee (2017) incorporated Markov decision process into genetic algorithms to formulate trading strategies for stock markets, which gave stock selection, market timing and capital allocation at the same time. Tang et al.(2019) investigated a new approach of integrating piecewise linear representation and weighted support vector machine for forecasting a stock turning point, considered as a period rather than a point.

However, there have been few AI papers to focus on a price formulation process driven by investors' trading activities, or demand/supply. One of the research topics with this perspective is agent-based artificial market modeling. For example, Cocco et al.(2019) attempted to reproduce a bitcoin price series with some stylized facts through an agent-based artificial market model. In this artificial market model, there existed two kinds of agents called Chartists and Random traders: Chartists followed a given set of technical trading rules selected by a genetic algorithm based on four technical indicators, while random traders trade without any strategy. Then, it was tested whether those trading simulations for two types of traders can reproduce a bitcoin price series equipped with the stylized facts. Let us note that the research on artificial market modeling has a similar structure, though there exist some important varieties including the assumption on types of traders.

This paper proposes a new scheme to explain market price dynamics generated from multiple agents' trading activities. Particularly, the current price changes are represented as a linear combination of daily trades by the multiple agents, based on an assumption that the asset prices are changing to resolve their excess demand/supply. Here, those traders are supposed to follow predetermined investment strategies, who are categorized into the three types; (1) trend-following traders, (2) contrarian (mean-reversion) traders and (3) yield curve-based equity traders.

As a helpful interpretation, the proposed price formulation equation stands for a factor decomposition model of the price changes with the three trading factors, where the coefficients,

the so-called factor loadings, denote the strength of price impact arising from the three types of trading. Especially, since those coefficients are thought to be unobservable time-varying variables, they need to be estimated for applying to financial practice. Then, this paper resorts to state space modeling for their sequential estimation.

State space models are commonly used in various fields (Arulampalam et al., 2002; Liu, Sun, 2012; Fileccia, Sgarra, 2018; Orchard, Vachtsevanos, 2009; Nakano et al., 2017a; Nakano et al., 2017b) to represent dynamic dependence between latent state and observed variables. Their dynamics are described as time-series models called state and observation equations. Moreover, Bayesian filtering algorithms make it possible to estimate the time transitions of unobservable state variables.

This paper makes use of this state-space approach by regarding the coefficients, i.e. factor loadings, as state variables, which are sequentially estimated through daily information updates. Especially, since contrarian (mean-reversion) traders (2) and yield curve-based equity traders (3), differently from trend-follower (1), attempt to detect a sign of trend conversion or market crises, new signals for proactive risk management can be introduced by using the filtering estimation results.

In empirical experiments with S&P500 futures and US 10 year treasury note futures, it is first confirmed that our proposed price formulation model successfully replicates the actual market price movements. Then, the systematic investigation using the estimated state variables is implemented to find new proactive risk management signals in the US stock market. As a result, it is found that the demands of yield curve-based traders subtracting those of trend-followers could be a promising signal of stock market crashes, which has successfully enhanced the simple buy-and-hold strategy of SP, as well as constant proportion strategies.

The remainder of this paper is organized as follows: First, Section 2 describes our proposed scheme to explain market dynamics from daily transactions of three types of traders. Then, after showing PF implementation and its results in Section 3, Section 4 illustrates our investment simulations with proposed new indicators. Finally, Section 5 concludes.

## 2 Methodology

This section first shows an overview of our proposed framework in Section 2.1. Then, after introducing the state-space model in Section 2.2, Section 2.3 presents a state-space representation of our proposed model. In Section 2.4, the investment strategies of three types of traders are explained.

### 2.1 Proposed framework

Let us consider a financial market, where  $M$ -financial assets are traded by  $N$ -types of traders with prices  $P_t \in \mathbb{R}^M$ . Each type of traders follows a predetermined investment strategy (e.g. trend-following), represented as mathematical functions  $\omega_t^{(i)} = f^{(i)}(X_t^{(i)})$ ,  $i = 1, \dots, N$ , where  $\omega_t^{(i)} \in \mathbb{R}^M$  denotes the output portfolio weights over a period  $[t, t + 1)$ , while  $X_t^{(i)}$  indicates the input variables of the trader- $(i)$ 's strategy calculated by price, volume and bond yield data until time  $t - 1$ .

Under those situations, market clearing prices  $(P_t)_t$  attaining demand/supply balances are supposed to satisfy the following dynamic (discrete-time) equilibrium equation:

$$\Delta P_t = \sum_{i=1}^N Z_t^{(i)} \Delta \omega_{t-1}^{(i)} + u_t, \quad (1)$$

where  $u_t$  is a random vector and  $\Delta P_t := P_t - P_{t-1}$ ,  $\Delta\omega_{t-1}^{(i)} := \omega_{t-1}^{(i)} - \omega_{t-2}^{(i)}$ . Let us notice that the price changes  $\Delta P_t \in \mathbb{R}^M$  are represented by a linear combination of the players' daily rebalance tradings  $(\Delta\omega_{t-1}^{(i)})_i \in \mathbb{R}^{M \times N}$  with the coefficients  $(Z_t^{(i)})_i \in \mathbb{R}^N$ . Here, the coefficient  $Z_t^{(i)} \in \mathbb{R}^+$  is interpreted as the strength of price impact arising from the  $i$ -th player's trading  $\Delta\omega_{t-1}^{(i)}$ , including the number or/and size of the  $i$ -th type of traders. We also note that Eq. (1) is a factor decomposition equation of the price changes  $\Delta P_t$  with factors  $(\Delta\omega_{t-1}^{(i)})_i$  and factor loadings  $(Z_t^{(i)})_i$ . In addition, it is an important implication of Eq. (1) that the prices changes  $\Delta P_t$  are formulated to resolve excess demand/supply at date  $t - 1$  generated by each player's portfolio rebalancing trade  $(\Delta\omega_{t-1}^{(i)})_i$ .

Then, based on  $\Delta P_t$  and  $(\Delta\omega_{t-1}^{(i)})_i$  observable at date- $t$ , the coefficients  $(Z_t^{(i)})_i$  are estimated as hidden time-varying variables to satisfy Eq. (1) through a state-space approach. Especially, the current paper exploits Monte-Carlo simulation-based filtering algorithm, the so-called particle filter (PF), because it enables us to sequentially estimate the time-varying factor loadings  $Z_t^{(i)}$  with low computational complexity under non-Gaussian and non-linear setting. Let us recall that since the  $(Z_t^{(i)})_i$  values are limited to positive real numbers, i.e.  $Z_t^{(i)} \in \mathbb{R}^+$ , standard analytical linear filtering algorithms such as Kalman filter are not applicable. This restriction on  $Z_t^{(i)}$  is required, because the position increase  $\Delta\omega_{t-1}^{(i)} > 0$  should cause the asset price to increase  $\Delta P_{t-1} > 0$  based on the fundamental relation between demand/supply and price, which is also helpful to preserve the interpretation of  $(Z_t^{(i)})_i$  as the number/size of the  $i$ -th type of traders.

Moreover, in Section 4.1, we will introduce a new indicator ( $\eta_t$ ) for proactive risk management using the estimated state variables, whose effectiveness will be shown in investment simulations with empirical data of US stock market index.

Finally, Fig. 1 illustrates a flowchart of our proposed scheme for proactive risk management, whose detailed setting will be introduced in subsequent sections. As shown in Fig. 1, our PF algorithm sequentially estimates the unobservable state variables  $(Z_t^{(i)})_i$  for a given current change  $\Delta P_t$  and a given current trading  $\Delta\omega_{t-1}^{(i)}$  calculated by the past information. Then, based on those estimated  $(Z_t^{(i)})_i$ , a new indicator  $\eta_t$  for risk proactive management at date  $t$  is defined, yielding investment decision at date  $t + 1$  to confirm out-of-sample performance evaluations.

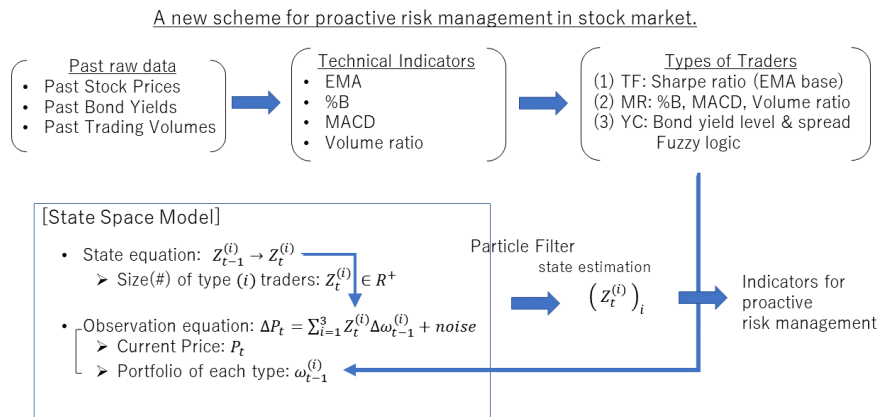


Fig. 1: Overview of our proposed scheme

## 2.2 State-space model

A state space framework assumes that there exist unobservable latent/state variables driven by stochastic processes behind observed time-series data. Precisely, it consists of the following observation and state equations.

$$O_t = H(Z_t, u_t), \quad [\text{observation equation}] \quad (2)$$

$$Z_t = G(Z_{t-1}, v_t), \quad [\text{state equation}] \quad (3)$$

where  $O_t$  and  $Z_t$  are a vector of observable and latent/state variables, respectively. Besides,  $u_t$  and  $v_t$  denote random variables for observation and state transition, respectively. Here, the functions  $H$  and  $G$  are non-linear functions in general.

Bayesian filtering technique is an on-line statistical approach to sequentially estimate the state variables  $Z_t$  through the observed data until time  $t$ ,  $O_{1:t} \equiv (O_1, \dots, O_t)$ , that is, to estimate the distribution  $p(Z_t|O_{1:t})$ . Importantly, filtering approaches are appropriate for reflecting dynamic changes of environment, because their estimation is updated for each time of new observation data arrival.

Particularly, particle filtering (PF) resorts to Monte Carlo simulation for the estimation of state variables, whereby it is applicable to non-linear and non-Gaussian settings. This generality is essential to apply PF to machine learning under various situations in practice. The detailed algorithm of our PF is described in Appendix.A.

## 2.3 Proposed state-space model

This section describes a state-space model to estimate the proposed market price determination model introduced in Section 2.1. As explained in Section 2.1, the daily tradings are executed according to  $N$ -patterns of investment strategies, represented by mathematical functions  $f^{(i)}$ ,  $i = 1, \dots, N$ . Precisely, the function  $f^{(i)}$  outputs a portfolio weight  $\omega_t^{(i)} = (\omega_{1,t}^{(i)}, \dots, \omega_{M,t}^{(i)}) \in \mathbb{R}^M$  at time  $t$  from a specific input vector  $X_t^{(i)}$  defined by the information accessible until time  $t$ , i.e.  $\omega_t^{(i)} = f^{(i)}(X_t^{(i)})$ .

Then, the following state-space model is introduced to express the asset price transitions driven by the  $N$ -types of tradings.

$$\Delta P_t = \sum_{i=1}^N Z_t^{(i)} \Delta \omega_{t-1}^{(i)} + u_t, \quad \omega_{t-1}^{(i)} = f^{(i)}(X_{t-1}^{(i)}), \quad [\text{observation eq.}] \quad (4)$$

$$Z_t^{(i)} = 1_{\{z_t^{(i)} > 0\}} z_t^{(i)}, \quad z_t^{(i)} = Z_{t-1}^{(i)} + v_t^{(i)}, \quad [\text{state eq.}] \quad (5)$$

where  $u_t = (u_{j,t})_j \in \mathbb{R}^M$  and  $v_t^{(i)} \in \mathbb{R}$  are random noises following normal distributions, i.e.  $u_{j,t} \sim N(0, \sigma_j^u)$  and  $v_t^{(i)} \sim N(0, \sigma_i^v)$ . Also, for a given set  $A$ ,  $1_A(x)$  denotes an indicator function, which takes one for  $x \in A$  and zero for  $x \notin A$ . Let us notice that in the state equation, Eq. (5), the state variables  $(Z_t^{(i)})_i$  follow random walk processes, whose values are restricted to positive real numbers,  $Z_t^{(i)} \in \mathbb{R}^+$ ,  $i = 1, \dots, N$ , as explained in Section 2.1.

In this state-space modes, the coefficients of traders' rebalance trading  $(\Delta \omega_{t-1}^{(i)})$  are regarded as time-varying unobservable state variables  $(Z_t^{(i)})$ . Namely, the implementation of a filtering algorithm reveals which investment strategy explains well the current market price changes. Further, if estimated states  $Z_t^{(i)}$  are drastically changing, there is a possibility that a significant structural change has occurred in market price determination.

Let us remark that this simple state-space modeling enables us to obtain a clear interpretation of the current price movements of financial markets in terms of multiple trading patterns, which is updated through PF-based sequential estimation. Also, the model extension including the introduction of different traders' types is easily implemented due to the simple model framework.

## 2.4 Model specification

This section specifies the traders' investment strategies given by the function  $f^{(i)}$ . First of all, this research employs two assets, S&P500 futures and US 10-year T-Note futures ( $M = 2$ ). Thereafter, we will abbreviate those assets as SP and TY, respectively. The price determination of US stock and bond markets has great importance, reflecting global financial investors' views.

Particularly, we will focus on the detection of turning points in SP dynamics from the estimation of individual trader's behavior. In recent years, it has often been observed in financial markets that upward trended changes of US stock prices suddenly collapse, which causes a significant impact on global investors' portfolios, as well as other financial asset prices. To overcome the difficulty, proactive risk management to detect a sign of a market crash has been increasingly important. In that sense, TY is regarded as a tool for risk hedge in this paper, whose price typically goes up when negative shocks on the stock market occur.

Based on that background, the current work employs the following three types of traders, i.e.  $N = 3$ , of which details are stated in Section 2.4.1, 2.4.2 and 2.4.3, respectively:

- (1) Trend Follower (TF)
- (2) Contrarian (CT)
- (3) Yield Curve-based Equity trader (YC)

The proposed state-space model intends to reveal which type of traders is dominant in the current market price changes. Especially, while Trend Followers decide their positions based on a risk-return indicator so as to follow a current trend of the stock price, non-Trend Followers (i.e., Contrarians and Yield Curve-based Equity traders) attempt to detect signs of trend conversions or market crises based on technical indicators on stock and yield curve of US treasuries. Then, it is assumed that the comparison of the demands between Trend Followers and non-Trend Followers, estimated from the current market movement, gives us a clue for a possible trend conversion, or market crashes.

Let us notice that since TY is regarded as a risk-hedging tool for SP in this work, the remaining amount of money is invested to TY after deciding SP position, i.e.  $\omega_{2,t}^{(i)} = 1 - \omega_{1,t}^{(i)}$ , where  $\omega_{1,t}^{(i)}$  and  $\omega_{2,t}^{(i)}$  are portfolio weights of SP and TY, respectively.

### 2.4.1 Trader (1): Trend Follower

As a trend-following investment strategy, this work adopts a simple Sharpe ratio-based strategy. That is, for a given expected return  $\bar{r}_t = (\bar{r}_{j,t})_j \in \mathbb{R}^M$  and variance  $\sigma_t^2 = (\sigma_{j,t}^2)_j \in \mathbb{R}^M$ , a portfolio weight  $\omega_t^{(1)} \in \mathbb{R}^M$  ( $M = 2$ ) is calculated as follow:

$$\begin{aligned}\omega_{1,t}^{(1)} &= \frac{1}{\gamma} \frac{\bar{r}_{1,t}}{\sigma_{1,t}}, \\ \omega_{2,t}^{(1)} &= 1 - \omega_{1,t}^{(1)},\end{aligned}\tag{6}$$

where  $\gamma$  is a risk-averse parameter set to be 0.5. Also, the indexes  $j = 1, 2$  correspond with SP and TY, respectively. That is, the function  $f_1$  is defined as  $\omega_t^{(1)} = f^{(1)}(X_t^{(1)})$ ,  $X_t^{(1)} := (\bar{r}_t, \sigma_t)$ .

Here, for time-series data of the asset returns  $r_t = (r_{j,t})_j \in \mathbb{R}^M$  ( $M = 2$ ), the expected return  $\bar{r}_t = (\bar{r}_{j,t})_{j=1,2} \in \mathbb{R}^2$  and variance  $\sigma_t^2 = (\sigma_{j,t}^2)_{j=1,2} \in \mathbb{R}^2$  are obtained based on an exponential moving average (EMA) method as follow:

$$\begin{aligned}\bar{r}_{j,t} &= \alpha r_{j,t-1} + (1 - \alpha)\bar{r}_{j,t-1} \\ \sigma_{j,t}^2 &= \alpha(r_{j,t-1} - \bar{r}_{j,t-1})^2 + (1 - \alpha)\sigma_{j,t-1}^2\end{aligned}\quad (7)$$

Let us note that  $\alpha$  is parameterized by  $\alpha = 2/(1 + 100)$ , which is the so-called 100-days EMA.

## 2.4.2 Trader (2): Contrarian

Contrarian trading is an investment strategy to capitalize the mean-reverting behaviour of market price dynamics. Specifically, this work implements a rule-based contrarian (mean-reversion) trading with technical indicators for SP to detect a sign of conversion of trended price movements.

This work uses the following three technical indicators  $X_t^{(2)} = (X_{1,t}^{(2)}, X_{2,t}^{(2)}, X_{3,t}^{(2)})$ :

- %B, Bollinger bands  $X_{1,t}^{(2)}$ : Bollinger bands denote two sigma ranges from moving average lines. It can be a signal of overpricing/underpricing to check whether a given asset price is within the Bollinger band or not. As a signal, the following %B  $X_{1,t}^{(2)}$  is often used:

$$\begin{aligned}X_{1,t}^{(2)} &= \frac{P_{1,t-1} - \underline{P}_{1,t-1}}{\bar{P}_{1,t-1} - \underline{P}_{1,t-1}}, \\ \bar{P}_{1,t-1} &= m_{1,t-1}^P + 2s_{1,t-1}^P, \quad \underline{P}_{1,t-1} = m_{1,t-1}^P - 2s_{1,t-1}^P, \\ m_{1,t-1}^P &= \frac{1}{100} \sum_{s=t-100}^{t-1} P_{1,s}, \\ s_{1,t-1}^P &= \sqrt{\frac{1}{100} \sum_{s=t-100}^{t-1} (P_{1,s} - m_{1,t-1}^P)^2}.\end{aligned}\quad (8)$$

That is, the %B above one (resp. below zero) is a sign of overpricing (resp. underpricing). Let us note that 100-day moving averages are used in this work, which is one of the standard specifications, as shown in Investopedia.

- Moving Average Convergence/Divergence (MACD)  $X_{2,t}^{(2)}$ : This indicator measures a momentum to upward (resp. downward) movement from downward (resp. upward).

$$\begin{aligned}X_{2,t}^{(2)} &= \bar{P}_{t-1}^{\beta_1} - \bar{P}_{t-1}^{\beta_2}, \\ \bar{P}_{t-1}^\beta &= \beta P_{t-1} + (1 - \beta)\bar{P}_{t-1}^\beta, \quad \beta = \beta_1, \beta_2,\end{aligned}\quad (9)$$

where  $\beta_1 = 2/(1 + 12)$  and  $\beta_2 = 2/(1 + 26)$ , i.e. 12-days EMA and 26-days EMA. The choice of EMA terms (12 days and 26 days) is standard, as shown in Investopedia. It is regarded as a buying (resp. selling) signal that a sign of MACD  $X_{2,t}^{(2)}$  switches from negative (resp. positive) to positive (resp. negative).

- Up/Down Volume Ratio (VR)  $X_{3,t}^{(2)}$ : This indicator represents the relative strength of buying against selling in terms of the trading volume, taking values from zero to one:

$$X_{3,t}^{(2)} = \frac{\sum_{s=t-25}^{t-1} Vol_s^U}{\sum_{s=t-25}^{t-1} Vol_s^U + \sum_{s=t-25}^{t-1} Vol_s^D}\quad (10)$$



where  $VolL_s^U$  and  $VolL_s^D$  represents trading volume of SP at time- $s$ , when  $P_{1,s} > P_{1,s-1}$  and  $P_{1,s} < P_{1,s-1}$ , respectively. It is assumed to be a buying (resp. selling) signal that if VR  $X_{3,t}^{(2)}$  rises above 0.7 (resp. drops below 0.3), which is a standard threshold setting.

Based on those technical indicators, the trader-(2), i.e. Contrarians, adopts the following rule-based investment with those technical indicators  $X_t^{(2)} = (X_{1,t}^{(2)}, X_{2,t}^{(2)}, X_{3,t}^{(2)})$  to capitalize the mean-reverting behavior of prices.

$$\begin{aligned}
\omega_{1,t}^{(2)} &= f^{(2)}(X_t^{(2)}) \\
&= 0.1 \\
&\quad + 1_{\{X_{1,t}^{(2)} < 0\}} \times 0.2 - 1_{\{X_{1,t}^{(2)} > 1\}} \times 0.2 \\
&\quad + 1_{\{X_{2,t}^{(2)} \geq 0.0\}} \times 0.1 - 1_{\{X_{2,t}^{(2)} < 0.0\}} \times 0.1 \\
&\quad + 1_{\{X_{3,t}^{(2)} < 0.3\}} \times 0.2 - 1_{\{X_{3,t}^{(2)} > 0.7\}} \times 0.2, \\
\omega_{2,t}^{(2)} &= 1 - \omega_{1,t}^{(2)}.
\end{aligned} \tag{11}$$

The position of the trader-(2) employs a traditional static strategy with a constant portfolio weight (0.1, 0.9) as a benchmark portfolio, which are adjusted based on the technical indicators (%B, MACD, VR) when they tell us buying/selling signals. Precisely, the trader-(2) increases the position of SP by 0.2/0.1/0.2 from the benchmark weight  $\omega_{1,t}^{(2)} = 0.1$ , when %B/MACD/VR shows a signal of price rising. Contrary, he reduces the position of SP by 0.2/0.1/0.2, when %B/MACD/VR shows a signal of price dropping. Let us note those types of traders, the so-called contrarian traders, are commonly observed in financial markets, who capitalize mean-reverting price movements based on signals perceived by those technical indicators.

Here, we also mention that the adjustment value is 0.1 only for MACD, though the others are set to be 0.2. Actually, MACD-based adjustment to the benchmark weight (0.1, 0.9) is active at any time, because its condition  $X_{2,t}^{(2)} \geq 0$  or  $X_{2,t}^{(2)} < 0$  always holds, while the adjustments by %B and VR are active only under limited situations, i.e.  $X_{1,t}^{(2)} > 1$ ,  $X_{1,t}^{(2)} < 0$  and  $X_{3,t}^{(2)} > 0.7$ ,  $X_{3,t}^{(2)} < 0.3$ , respectively. Also, let us notice that the trader-(2)'s SP position takes values from  $-0.4$  to  $0.6$ , as shown in Eq. (11). Actually, the portfolio functions  $f^{(i)}$ ,  $i = 1, 2, 3$  and those parameters are set so that portfolio returns, risks and weights of all the three types of traders take a similar range, which makes it easier to compare and interpret the results of state estimation among the traders (1)-(3). We remark that those tunings do not essentially deteriorate the performance measurement of our state-space approach, because the only increments  $\Delta\omega_t^{(i)}$ , not the levels of  $\omega_t^{(i)}$ , are related to price determination in our model. For those exogenously given the trading factors  $(\Delta\omega_t^{(i)})_i$ , their coefficients  $(Z_t^{(i)})_i$ , or factor loadings, are estimated as unobservable state variables to properly replicate the current price changes, as shown in Eq. (4).

### 2.4.3 Trader (3): Yield Curve-based Equity trading

Yield curves have been considered to be one of the most informative resources to predict the future of macroeconomics situations and financial markets, into which various professional views are incorporated (Nakano et al., 2018; Nakano et al., 2020) In particular, with the slight modification of BlackRock (2018), it is supposed that both of the level and slope of the yield curve are effective real-time business cycle indicators, which leads to the following four basic regimes:

- (i) Bear steepening; interest rates rising & yield curve steeper

- (ii) Bear flattening; interest rates rising & yield curve flattening
- (iii) Bull steepening; interest rates falling & yield curve steeper
- (iv) Bull flattening; interest rates falling & yield curve flattening

We suppose that the market sentiment in the US stock market has been strong from (i) to (iv) by analyzing the historical relationship over the last 20 years. In other words, the bear steepening regime (i) indicates the strongest risk-on signal, while the bull flattening (iv) shows a risk-off signal. Then, this paper refers to traders who use yield curve information to measure stock market sentiment as “Yield Curve-based Equity traders”. Let us notice that the target of this investment is SP, not yield curves themselves.

Based on this discussion, the current work introduces a Takagi-Sugeno fuzzy system (Takagi, Sugeno, 1985; Sugeno, Kang, 1988) for portfolio construction. Fuzzy system (Mamdani, Assilian, 1975) stores multiple IF-THEN inference rules with linguistic expressions called fuzzy sets (Zadeh, 1965; Zadeh, 1999), which enables to imitate human expert reasoning within a computer. Since the qualitative and intuitive explanation of a decision to stakeholders is an important task, fuzzy systems are appropriate for decision-making in financial markets (Nakano et al., 2017c; Nakano et al., 2017d; Takahashi, Takahashi, 2020). Specifically, the current work employs the following four IF-THEN rules, corresponding with the four phases (i)-(iv):

- (i) IF  $X_{1,t}^{(3)}$  is  $A_1^{high}$  and  $X_{2,t}^{(3)}$  is  $A_2^{high}$ , THEN a portfolio weight for SP  $\omega_{1,t}^{(3)} = 0.5$ ,
- (ii) IF  $X_{1,t}^{(3)}$  is  $A_1^{high}$  and  $X_{2,t}^{(3)}$  is  $A_2^{low}$ , THEN a portfolio weight for SP  $\omega_{1,t}^{(3)} = 0.3$ ,
- (iii) IF  $X_{1,t}^{(3)}$  is  $A_1^{low}$  and  $X_{2,t}^{(3)}$  is  $A_2^{high}$ , THEN a portfolio weight for SP  $\omega_{1,t}^{(3)} = 0.1$ ,
- (iv) IF  $X_{1,t}^{(3)}$  is  $A_1^{low}$  and  $X_{2,t}^{(3)}$  is  $A_2^{low}$ , THEN a portfolio weight for SP  $\omega_{1,t}^{(3)} = -0.1$ ,

where  $X_{1,t}^{(3)}$  and  $X_{2,t}^{(3)}$  corresponds with US 2y yield levels and the difference between US 10y and 2y yields at date  $t - 1$ , respectively. Also,  $A_1^{high}$  and  $A_1^{low}$  are fuzzy sets for  $X_{1,t}^{(3)}$ , i.e. US 2y yield levels, which means  $A_1^{high}$  and  $A_1^{low}$  measure interest rate rising and falling, respectively. As well,  $A_2^{high}$  and  $A_2^{low}$  are fuzzy sets for  $X_{2,t}^{(3)}$ , i.e. the difference between US 10y yield and US 2y yield, which implies that  $A_2^{high}$  and  $A_2^{low}$  measure yield curve steepening and flattening, respectively.

Moreover, the following Gaussian membership functions are used, which measures how ”high” or ”low” from historical one-year data:

$$\begin{aligned}\mu^{high}(X_{k,t}^{(3)}) &= \exp\left(-\frac{(X_{k,t}^{(3)} - \overline{X}_{k,t-1}^{(3)})^2}{\Sigma_{k,t-1}}\right), \\ \mu^{low}(X_{k,t}^{(3)}) &= \exp\left(-\frac{(X_{k,t}^{(3)} - \underline{X}_{k,t-1}^{(3)})^2}{\Sigma_{k,t-1}}\right),\end{aligned}\tag{12}$$

where

$$\begin{aligned}\overline{X}_{k,t-1}^{(3)} &= \max_{s=t-250, \dots, t-1} \{X_{k,s}^{(3)}\}, \\ \underline{X}_{k,t-1}^{(3)} &= \min_{s=t-250, \dots, t-1} \{X_{k,s}^{(3)}\}, \\ \Sigma_{k,t-1} &= 0.5 \times (\overline{X}_{k,t-1}^{(3)} - \underline{X}_{k,t-1}^{(3)}).\end{aligned}\tag{13}$$

Then, the firing strength of the rules  $M_t^1, \dots, M_t^4$  is calculated as follows:

$$\begin{aligned}
M_t^1 &= \mu^{high}(X_{1,t}^{(3)}) \times \mu^{high}(X_{2,t}^{(3)}), \\
M_t^2 &= \mu^{high}(X_{1,t}^{(3)}) \times \mu^{low}(X_{2,t}^{(3)}), \\
M_t^3 &= \mu^{low}(X_{1,t}^{(3)}) \times \mu^{high}(X_{2,t}^{(3)}), \\
M_t^4 &= \mu^{low}(X_{1,t}^{(3)}) \times \mu^{low}(X_{2,t}^{(3)}).
\end{aligned} \tag{14}$$

Thereby, the yield curve-based equity traders decide their portfolio weight based on Takagi-Sugeno zero-order fuzzy model as follows:

$$\begin{aligned}
\omega_{1,t}^{(3)} &= \frac{M_t^1 \times 0.5 + M_t^2 \times 0.3 + M_t^3 \times 0.1 + M_t^4 \times (-0.1)}{M_t^1 + M_t^2 + M_t^3 + M_t^4}, \\
\omega_{2,t}^{(3)} &= 1 - \omega_{1,t}^{(3)}.
\end{aligned} \tag{15}$$

### 3 Estimation

This section explains estimation settings and results to validate our proposal. After explaining the setup, the results of PF estimation are shown.

#### 3.1 Dataset

Our dataset is summarized as follows, where the data source is Bloomberg:

- SP: S&P 500 futures price daily data, which are generated by rolling futures with the first contract month. Bloomberg ticker code is SP1 PX\_LAST.
- TY: US 10-year treasury note futures price daily data, which are generated by rolling the futures with the first contract month. Bloomberg ticker code is TY1 PX\_LAST.
- Trading Volume of SP: Daily trading volume data of S&P 500 futures with the first contract month. Bloomberg ticker code is SP1 PX\_VOLUME.
- US 2y yields: Daily US 2-year yield data. Bloomberg ticker code is GT2 Govt PX\_MID.
- US 10y yields: Daily US 10-year yield data. Bloomberg ticker code is GT10 Govt PX\_MID.

Here, the data period is from 1990/2/5 to 2020/4/9. Let us notice that our SP and TY are futures, which implies those returns are excess returns. Namely, it is not necessary to subtract funding costs or a risk-free rate in performance evaluation such as Sharpe ratio.

#### 3.2 Setting of particle filter

As stated in the previous Section 3.1, our data period is over 1990/2/5-2020/4/9. However, about the first three years are regarded as a training period, which means the investment simulation period is over 1992/12/23-2020/4/9. To implement PF, the parameters are set as follows:

- Standard deviation of the noise in the observation equation:  $(\sigma_{1,t}^u, \sigma_{2,t}^u) = (0.02, 0.005)$ ,
- Standard deviation of noises in the state equations:  $(\sigma_{i,t}^v) = 0.025$ ,  $i = 1, 2, 3$
- Number of particles in PF:  $L = 100,000$

For the standard deviation of noises in the observation equation, since we use price data normalized as  $P_{1,0} = P_{2,0} = 1$ , those specifications make sense.

### 3.3 Result of estimation

Fig. 2 has scattered the SP price process  $(P_{1,t})_t$  and its replication  $(\hat{P}_{1,t})_t$  obtained by the state estimation as follows:

$$\hat{P}_{1,t} = P_{1,t-1} + \sum_{i=1}^3 \hat{Z}_t^{(i)} \Delta\omega_{1,t-1}^{(i)}. \quad (16)$$

As observed in Fig. 2, the replication has been successfully attained. Also, Fig. 3 displays 250-days EMA of estimated demand  $(\hat{Z}_t^{(i)} \Delta\omega_{1,t-1}^{(i)})_{i=1,2,3}$ , respectively.

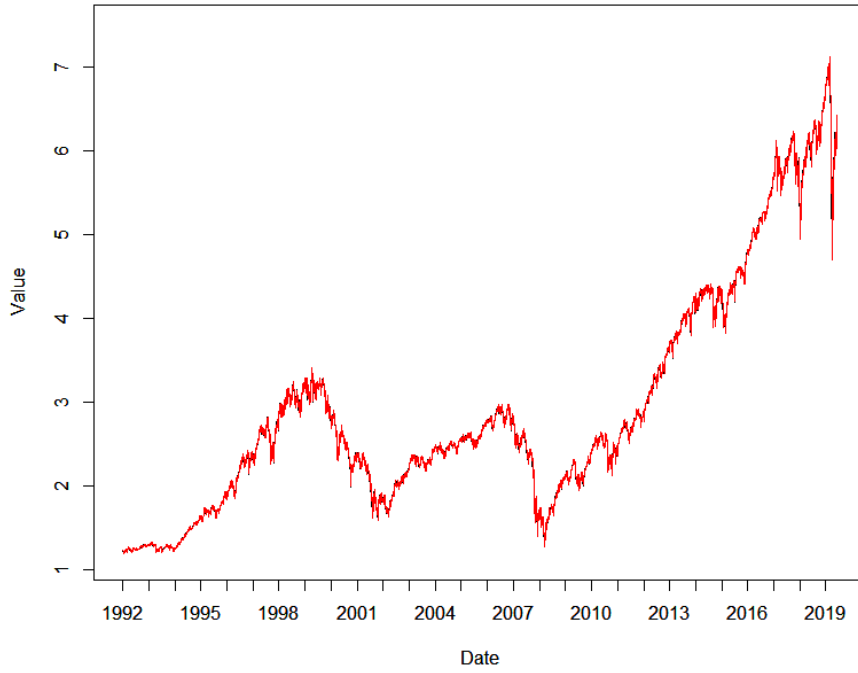


Fig. 2: SP (black line) & Replicated SP (red line)

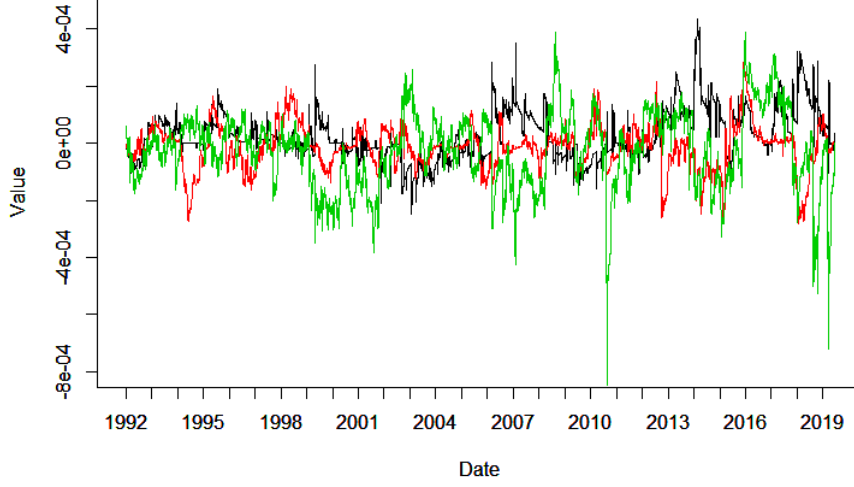


Fig. 3: 250-day EMA of estimated demand  $(\hat{Z}_t^{(i)} \Delta \omega_{1,t-1}^{(i)})_{i=1,2,3}$ : Contrarian(black line), Yield Curve-based Equity trader(red line), Trend Follower(green line).

## 4 Application to proactive investment risk management

In this section, Section 4.1 introduces new signals for proactive risk management. Then, after explaining a setup on our investment simulations in Section 4.2, the result is shown.

### 4.1 New indicator

This work searches various patterns of investment simulations to obtain effective risk management signals based on our proposed scheme. First, let us remind that the following variables  $\xi_t^{(i)}$ ,  $i = 1, 2, 3$  can be interpreted as aggregate demands or rebalancing transactions on SP for each type of traders (1)-(3).

$$\xi_t^{(i)} := \hat{Z}_t^{(i)} \Delta \omega_{1,t-1}^{(i)} \quad (17)$$

where  $\hat{Z}_t^{(i)}$ ,  $i = 1, 2, 3$  are state variables estimated by particle filtering algorithm.

Since those variables  $\xi_t^{(i)}$ ,  $i = 1, 2, 3$  drastically change, we employ their EMA and MACD for risk management signals:

- EMA:  $\bar{\xi}_{t,k}^{(i)} := \beta_k \xi_t^{(i)} + (1 - \beta_k) \bar{\xi}_{t-1,k}^{(i)}$ ,  $i = 1, 2, 3$ ,  $k = 1, 2$
- MACD:  $\bar{\xi}_{t,1}^{(i)} - \bar{\xi}_{t,2}^{(i)}$ ,

where  $\beta_1 = 2/(1 + 100)$  and  $\beta_2 = 2/(1 + 250)$ , i.e. 100-days EMA and 250-days EMA. Using those EMAs and MACDs, the 24 patterns of indicators are introduced in simple investment simulations, as shown in Table 1.

Table 1: Indicators

	input	content
(I1)	$\bar{\xi}_{t,1}^{(1)}$	TF(100-day EMA)
(I2)	$\bar{\xi}_{t,1}^{(2)}$	CT(100-day EMA)
(I3)	$\bar{\xi}_{t,1}^{(3)}$	YC(100-day EMA)
(I4)	$\bar{\xi}_{t,2}^{(1)}$	TF(250-day EMA)
(I5)	$\bar{\xi}_{t,2}^{(2)}$	CT(250-day EMA)
(I6)	$\bar{\xi}_{t,2}^{(3)}$	YC(250-day EMA)
(I7)	$\bar{\xi}_{t,1}^{(2)} + \bar{\xi}_{t,1}^{(3)} - \bar{\xi}_{t,1}^{(1)}$	CT+YC-TF(100-day EMA)
(I8)	$\bar{\xi}_{t,2}^{(2)} + \bar{\xi}_{t,2}^{(3)} - \bar{\xi}_{t,2}^{(1)}$	CT+YC-TF(250-day EMA)
(I9)	$\bar{\xi}_{t,1}^{(2)} + \bar{\xi}_{t,1}^{(3)} - 2\bar{\xi}_{t,1}^{(1)}$	CT+YC-2*TF(100-day EMA)
(I10)	$\bar{\xi}_{t,2}^{(2)} + \bar{\xi}_{t,2}^{(3)} - 2\bar{\xi}_{t,2}^{(1)}$	CT+YC-2*TF(250-day EMA)
(I11)	$\bar{\xi}_{t,1}^{(2)} - \bar{\xi}_{t,1}^{(1)}$	CT-TF(100-day EMA)
(I12)	$\bar{\xi}_{t,1}^{(3)} - \bar{\xi}_{t,1}^{(1)}$	YC-TF(100-day EMA)
(I13)	$\bar{\xi}_{t,2}^{(2)} - \bar{\xi}_{t,2}^{(1)}$	CT-TF(250-day EMA)
(I14)	$\bar{\xi}_{t,2}^{(3)} - \bar{\xi}_{t,2}^{(1)}$	YC-TF(250-day EMA)
(I15)	$\bar{\xi}_{t,1}^{(2)} + \bar{\xi}_{t,1}^{(3)}$	CT+YC(100-day EMA)
(I16)	$\bar{\xi}_{t,2}^{(2)} + \bar{\xi}_{t,2}^{(3)}$	CT+YC(250-day EMA)
(I17)	$\bar{\xi}_{t,1}^{(2)} - \bar{\xi}_{t,2}^{(2)}$	CT(100-day EMA)-CT(250-day EMA)
(I18)	$\bar{\xi}_{t,1}^{(3)} - \bar{\xi}_{t,2}^{(3)}$	YC(100-day EMA)-YC(250-day EMA)
(I19)	$\bar{\xi}_{t,1}^{(1)} - \bar{\xi}_{t,2}^{(1)}$	TF(100-day EMA)-TF(250-day EMA)
(I20)	$(\bar{\xi}_{t,1}^{(2)} + \bar{\xi}_{t,1}^{(3)}) - (\bar{\xi}_{t,2}^{(2)} + \bar{\xi}_{t,2}^{(3)})$	(CT+YC)(100-day EMA) - (CT+YC)(250-day EMA)
(I21)	$(\bar{\xi}_{t,1}^{(2)} - \bar{\xi}_{t,1}^{(1)}) - (\bar{\xi}_{t,2}^{(2)} - \bar{\xi}_{t,2}^{(1)})$	(CT-TF)(100-day EMA) - (CT-TF)(250-day EMA)
(I22)	$(\bar{\xi}_{t,1}^{(3)} - \bar{\xi}_{t,1}^{(1)}) - (\bar{\xi}_{t,2}^{(3)} - \bar{\xi}_{t,2}^{(1)})$	(YC-TF)(100-day EMA) - (YC-TF)(250-day EMA)
(I23)	$(\bar{\xi}_{t,1}^{(2)} + \bar{\xi}_{t,1}^{(3)} - \bar{\xi}_{t,1}^{(1)}) - (\bar{\xi}_{t,2}^{(2)} + \bar{\xi}_{t,2}^{(3)} - \bar{\xi}_{t,2}^{(1)})$	(CT+YC-TF)(100-day EMA)-(CT+YC-TF)(250-day EMA)
(I24)	$(\bar{\xi}_{t,1}^{(2)} + \bar{\xi}_{t,1}^{(3)} - 2\bar{\xi}_{t,1}^{(1)}) - (\bar{\xi}_{t,2}^{(2)} + \bar{\xi}_{t,2}^{(3)} - 2\bar{\xi}_{t,2}^{(1)})$	(CT+YC-2*TF)(100-day EMA)-(CT+YC-2*TF)(250-day EMA)

Then, it is tested to improve a simple buy-and-hold strategy of SP  $\omega_t = (1, 0)$  by cutting its position, when those indicators satisfy given conditions. As the conditions, the following 6 patterns are tested.

- (C1) SP position is cut over the period  $\eta_t < b_t$
- (C2) SP position is cut over the period  $\eta_t > b_t$
- (C3) SP position is cut over the period  $b_{-,t} < \eta_t < b_{+,t}$
- (C4) SP position is cut over the period  $\eta_t > b_{+,t}, \eta_t < b_{-,t}$
- (C5) SP position is cut one day after  $\eta_t$  goes across the threshold  $b_{+,t}$  from above to below ( $\eta_{t-1} > b_{+,t}, \eta_t < b_{+,t}$ ), whose position cut is continued one day after  $\eta_t$  goes below  $b_{-,t}$  for the first time.
- (C6) SP position is cut one day after  $\eta_t$  goes across the threshold  $b_{-,t}$  from below to above ( $\eta_{t-1} < b_{-,t}, \eta_t > b_{-,t}$ ), whose position cut is continued one day after  $\eta_t$  goes above  $b_{+,t}$  for the first time,

where  $\eta_t$  is a generic expression of the indicators listed in Table 1. As well,  $b_+, b_-, b$  are threshold values to decide the position cut, in which the following cases are tested.

$$\begin{aligned}
\text{(B1)} \quad & b_{+,t} \in B_+ := \{0, 0.00001, 0.00005, 0.0001, 0.000125, 0.00015, 0.0002\}, \\
& b_{-,t} \in B_- := \{0, -0.00001, -0.00005, -0.0001, -0.000125, -0.00015, -0.0002\}, \\
& b_t \in B := B_+ \cup B_-
\end{aligned}$$

$$\begin{aligned}
\text{(B2)} \quad & b_{+,t} \in B_+ := \{0, 0.25\sigma_t^\eta, 0.5\sigma_t^\eta, \sigma_t^\eta, 2\sigma_t^\eta\}, \\
& b_{-,t} \in B_- := \{0, -0.25\sigma_t^\eta, -0.5\sigma_t^\eta, -\sigma_t^\eta, -2\sigma_t^\eta\}, \\
& b_t \in B := B_+ \cup B_-
\end{aligned}$$

where  $\sigma_t^\eta$  denotes sample standard deviations of the past one year of  $(\eta_t)$ ,  $\eta_{t-250}, \dots, \eta_{t-1}$ .

In addition, we test two cases on investment assets over the periods of SP position cut, i.e. the cash and TY, which are called by SP-Cash and SP-TY, or just Cash and TY, respectively. Let us note that the cash return is assumed to be zero.

Overall, for the 24 patterns of the indicators (I1)-(I24) summarized in Table 1, the 6 types of investment rules (C1)-(C6) are applied with the thresholds  $b_+, b_-, b$ , whose two values are selected from (B1) or (B2). Moreover, there are two cases that the SP position is shifted to Cash or TY. Hereafter, each case is labeled by connecting those four attributes, i.e. TY or Cash, (I1)-(I24), (C1)-(C6) and (B1)-(B2), with hyphens.

For instance, the case TY-(I1)-(C1)-(B1-2+) represents that

SP position is cut and shifted to TY, over the period during  $\xi_{t,1}^{(1)} < 0.00001$ ,

where (B1-2+) stands for the 2nd value in the set  $B_+$  for (B1), i.e.  $b_t = 0.00001$ . As well, the case Cash-(I14)-(C5)-(B2-5+&1-) represents that

SP position is cut and shifted to the cash, one day after  $\bar{\xi}_{t,2}^{(2)} - \bar{\xi}_{t,2}^{(1)}$  goes across the threshold  $b_{+,t} = 2\sigma_t^\eta$  from above to below, whose position cut is continued one day after  $\bar{\xi}_{t,2}^{(2)} - \bar{\xi}_{t,2}^{(1)}$  goes below  $b_{-,t} = 0$  for the first time,

where (B2-5+&1-) means that the fifth value of  $B_+$  and the first value of  $B_-$  in the case (B2), i.e.  $2\sigma_t^\eta$  and 0, are used as  $b_{+,t}$  and  $b_{-,t}$ .

At the end of this section, we emphasize that our investment strategies are implemented under the out-of-sample environment. That is,  $\eta_t$ , as well as  $b_{+,t}$ ,  $b_{-,t}$  and  $b_t$ , are calculated by the information up to the time  $t - 1$ .

## 4.2 Setting of investment simulation

Let us introduce the definition of the portfolio values  $\{V_t\}_{t=0, \dots, T}$  and investment returns  $\{R_t\}_{t=1, \dots, T}$  for given portfolio weight series  $(\omega_t)_t$  as follows.

$$V_{t+1} = V_t \left( 1 + \sum_{j=1}^M \omega_{j,t} r_{j,t+1} - \sum_{j=1}^M c_j |\omega_{j,t} - \omega_{j,t-1}| \right) \tag{18}$$

$$R_{t+1} = V_{t+1}/V_t - 1, \tag{19}$$

where the initial portfolio value is normalized to one, i.e.  $V_0 = 1$ . As well,  $c_j$  denotes the rate of transaction costs. That is, the current work regards the term  $\sum_{j=1}^M c_j |\omega_{j,t} - \omega_{j,t-1}| V_t$  as transaction costs, where  $|\omega_{j,t} - \omega_{j,t-1}| V_t$  is considered as trading volume. Also, let us note that the cash return is supposed to be zero.

Then, we also introduce performance ratios to evaluate performances of investment strategies, which are typically used in asset management practice. For time-series of investment returns  $(R_t)_{t=1, \dots, T}$  and portfolio values  $(V_t)_{t=0 \dots T}$ , the performance ratios are defined as follows:

- Average Return (AR): It is an annualized average of investment returns  $(R_t)_t$

$$AR = \frac{250}{T} R_t, \quad (20)$$

where the number "250" is for annualization.

- Standard Deviation (SD), Downside Deviation (DD): SD is a well-known investment risk measure defined as the annualized standard deviation of  $\{R_t\}$ , while DD only regards negative returns as risks.

$$SD \equiv \left\{ \frac{250}{T} \sum_{t=1}^T (R_t - \bar{R})^2 \right\}^{1/2}, \quad DD \equiv \left\{ \frac{250}{T} \sum_{t=1}^T \min(0, R_t)^2 \right\}^{1/2}, \quad \bar{R} \equiv \frac{1}{T} \sum_{t=1}^T R_t. \quad (21)$$

- Maximum drawdown (MDD): It is a max value in drawdowns realized in a given investment horizon  $[0, T]$ , where a drawdown is defined as a decline from the past peak value  $M_t$  to the present value  $V_t$  at each time  $t$ .

$$MDD = \max_{1 \leq t \leq T} \frac{M_t - V_t}{M_t}, \quad M_t = \max_{0 \leq s \leq t} V_s. \quad (22)$$

Shortly, MDD tells us the worst scenario for a given investment horizon, which means how much loss an investor suffers from if he/she enters and exits from an investment at the worst timing. As it is widely recognized in practice that investment performance largely depends on its starting and exiting timing, MDD is thought to be an important measure. Namely, a small MDD implies that an investor has not suffered from a large loss, whenever he/she starts the investment, at least on the past data.

- Sharpe ratio (ShR):

$$ShR = AR/SD. \quad (23)$$

In asset management theory and practice, risk-adjusted returns are well-known to represent a "true" investment performance. Among them, ShR is the most famous one, which is also a basic quantity in the field of financial economics. Let us remark that since we have already taken into account funding costs in raw return data as stated in Section 3.1, we don't subtract a risk-free rate from  $\bar{R}$  in the ShR definition.

- Sortino ratio (SoR): It is also useful because it adjusts risk by using the downside deviation (DD), which makes it possible to focus on only downside risks.

$$SoR = AR/DD. \quad (24)$$

- Sterling Ratio (StR): StR is a measure of risk-adjusted returns that use a drawdown measure as a denominator. We adopt the following definition:

$$StR = AR/MDD. \quad (25)$$

### 4.3 Result of investment

This section describes performances of our proposals in out-of-sample investment simulations. First of all, Table 2 illustrates the performance ratios of the traders (1)-(3), TF, CT and YC, whose performances are within a similar range, as explained in Section 2.4.



Table 4, Table 5 and Fig.4 show the two cases with the best performances, i.e. (I14)-(C6)-(B1-4+&3-) and (I12)-(C6)-(B2-1+&5-). That is, in the cases of position shift to the cash, Cash-(I14)-(C6)-(B1-4+&3-) attains the highest Sharpe ratio, while TY-(I12)-(C6)-(B2-1+&5-) does in the cases of position shift to TY ( US 10-year T-Note futures). Let us notice that although this work selects the best cases in terms of Sharpe ratio, the selection based on other criteria such as Sortino ratio, Sterling ratio, maximum drawdown and those mixtures are also possible. Here, the case Cash-(I14)-(C6)-(B1-4+&3-) represents

SP position is cut, shifted to the cash, one day after  $\bar{\xi}_{t,2}^{(3)} - \bar{\xi}_{t,2}^{(1)}$  goes across the threshold  $b_{+,t} = 0.0001$  from above to below, whose position cut is continued one day after  $\bar{\xi}_{t,2}^{(3)} - \bar{\xi}_{t,2}^{(1)}$  goes below  $b_{-,t} = -0.00005$  for the first time.

As well, the case TY-(I12)-(C6)-(B2-1+&5-) stands for

SP position is cut, shifted to the cash, one day after  $\bar{\xi}_{t,1}^{(3)} - \bar{\xi}_{t,1}^{(1)}$  goes across the threshold  $b_{+,t} = 0$  from above to below, whose position cut is continued one day after  $\bar{\xi}_{t,1}^{(3)} - \bar{\xi}_{t,1}^{(1)}$  goes below  $b_{-,t} = -2\sigma_t^\eta$  for the first time.

Hereafter, those two cases, (I14)-(C6)-(B1-4+&3-) and (I12)-(C6)-(B1-1+&5-), are called ‘‘Cash-Best’’ and ‘‘TY-Best’’ for simplicity.

The risk-adjusted returns (Sharpe ratio and Sortino ratio) of our proposed models successfully outperform the long-only strategies of SP and TY, shown in Table 3. Since  $\bar{\xi}_{t,1}^{(3)}, \bar{\xi}_{t,2}^{(3)}$  and  $\bar{\xi}_{t,1}^{(1)}, \bar{\xi}_{t,2}^{(1)}$  represent the aggregate demands of YC-based equity traders and TF traders, respectively, this result implies the behavior of YC-based traders relative to TF traders could be an important signal for SP price changes. Moreover, both cases recommend us that SP prices could drop when SP position of the YC-based traders relative to TF traders decreases from positive to negative. Thus, our proposed scheme has led us to new knowledge discovery, showing the importance of relative demand changes of the different two types of traders. In other words, it could be an effective signal to possible stock market crashes that net positions of YC-based traders, i.e. the demands of YC-based traders subtracting those of TF traders are dropping from positive to negative.

As well, Fig. 5-10 illustrate that our proposals, both of Cash-(I14)-(C6)-(B1-4+&3-) and TY-(I12)-(C6)-(B2-1+&5-), successfully avoid serious drawdowns in the IT bubble crash, Lehman shock and COVID-19 shock. That is, Fig. 5-7 (resp. Fig. 8-10) show cumulative returns of SP and Cash-(I14)-(C6)-(B1-4+&3-) (resp. TY-(I12)-(C6)-(B2-1+&5-)) for the three periods, i.e. 1992-2002, 2002-2012 and 2012-2021, which periods include IT bubble crash, Lehman shock and COVID-19 shock, respectively.<sup>1</sup> In particular, although the drawdown of the COVID-19 shock starting from February 2020 was much sharper than the other crises, our strategies suffer no losses thanks to our correct predictions.

In addition, a possible interpretation of the high performance of those combinations, i.e. the indicators (I12)/(I14) with the position cut condition (C6), is summarized as follows: First, the YC-based equity traders cut their SP positions, recognizing a sign of market crashes through the observing of yield-curve movement, which makes the indicators  $\eta_t = \bar{\xi}_{t,2}^{(3)} - \bar{\xi}_{t,2}^{(1)}$  or  $\eta_t = \bar{\xi}_{t,1}^{(3)} - \bar{\xi}_{t,1}^{(1)}$  go across the threshold values  $b_{+,t}$  from above to below resulting in SP position cut. Then, in the cases that a downtrend price change continues,  $\eta_t$  does not go across the lines  $b_{-,t}$  from above

<sup>1</sup>Thanks to anonymous referee’s suggestion, the figures for the third period, i.e., Fig. 7 and Fig. 10, are illustrated until 2021/12/31 to confirm that the proposed risk management signals, i.e., ‘‘Cash-Best’’ and ‘‘TY-Best’’ selected from the original data period 1990/2/5-2020/4/9, still work over the rebounding period of the US stock market after the COVID-19 shock.

to below soon, because the second terms of those indicators for trend-follower,  $\bar{\xi}_{t,1}^{(1)}$  and  $\bar{\xi}_{t,2}^{(1)}$ , get smaller, implying a prolonged period of SP position cut. On the contrary, when an uptrend price movement appears,  $\eta_t$  quickly goes across the lines  $b_{-,t}$  from above to below, implying an early termination of SP position cut.

Table 2: Performance ratios: Trader (1)-(3)

	TF	CT	YC
Average Return(per annum)	3.2%	4.1%	3.7%
Standard Deviation (per annum)	7.4%	6.0%	5.7%
Downside Deviation (per annum)	5.5%	4.2%	4.1%
Maximum Drawdown	16.9%	10.7%	10.7%
Sharpe ratio (per annum)	0.47	0.70	0.67
Sortino ratio (per annum)	0.63	1.00	0.93
Sterling ratio (per annum)	0.20	0.39	0.20

Table 3: Performances: SP, TY

	SP	TY
Average Return (per annum)	6.0%	3.6%
Standard Deviation (per annum)	18.5%	5.8%
Downside Deviation (per annum)	13.4%	4.1%
Maximum Drawdown	62.9%	13.7%
Sharpe ratio (per annum)	0.41	0.64
Sortino ratio (per annum)	0.56	0.90
Sterling ratio (per annum)	0.12	0.27

Table 4: Performance Ratio: (I14)-(C6)-(B1-4+&3-)

	Cash	TY
Average Return (per annum)	8.2%	10.8%
Standard Deviation (per annum)	10.3%	11.2%
Downside Deviation (per annum)	7.4%	8.0%
Maximum Drawdown	20.1%	20.1%
Sharpe ratio (per annum)	0.81	0.97
Sortino ratio (per annum)	1.13	1.35
Sterling ratio (per annum)	0.42	0.54

Table 5: Performance Ratio: (I12)-(C6)-(B1-1+&5-)

	Cash	TY
Average Return (per annum)	4.5%	8.1%
Standard Deviation (per annum)	5.9%	7.9%
Downside Deviation (per annum)	4.1%	5.5%
Maximum Drawdown	10.6%	13.7%
Sharpe ratio (per annum)	0.77	1.02
Sortino ratio (per annum)	1.11	1.47
Sterling ratio (per annum)	0.43	0.59

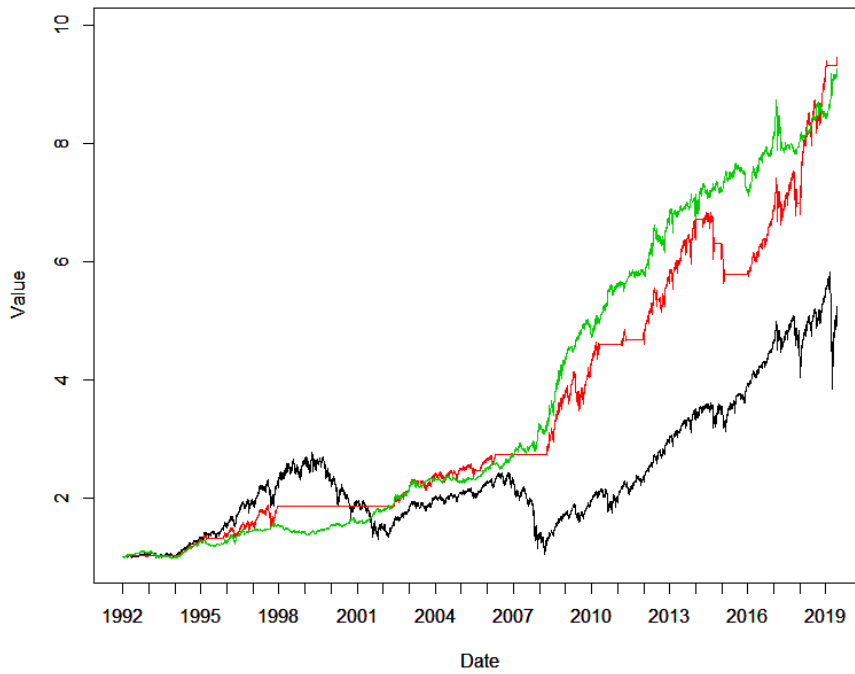


Fig. 4: Total Period: SP(black), Cash-(I14)-(C6)-(B1-4+&3-) (red), TY-(I12)-(C6)-(B1-1+&5-)(green)

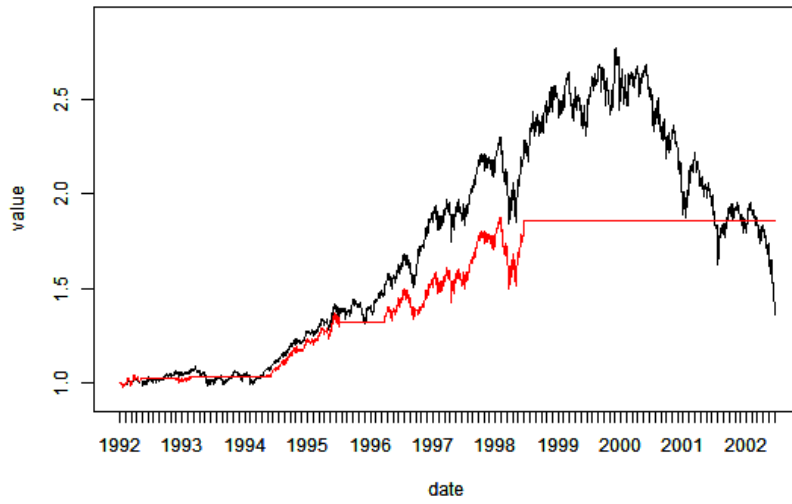


Fig. 5: 1992-2002: SP(black), Cash-(I14)-(C6)-(B1-4+&3-) (red)

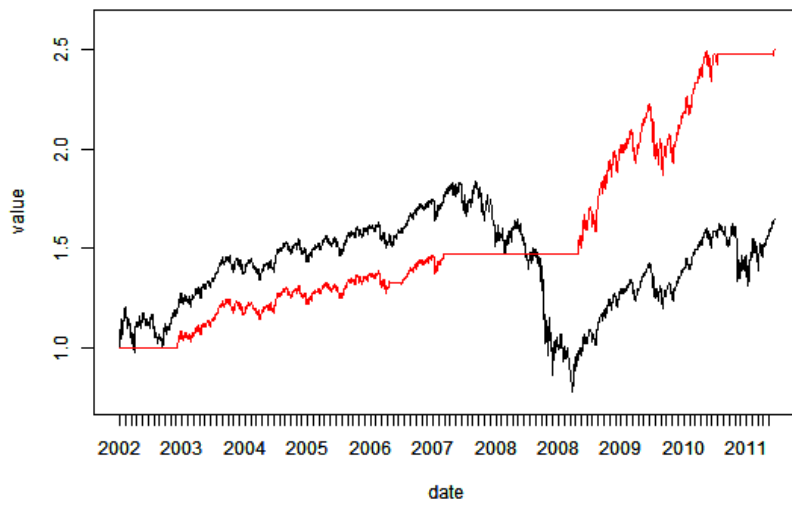


Fig. 6: 2002-2011: SP(black), Cash-(I14)-(C6)-(B1-4+&3-) (red)

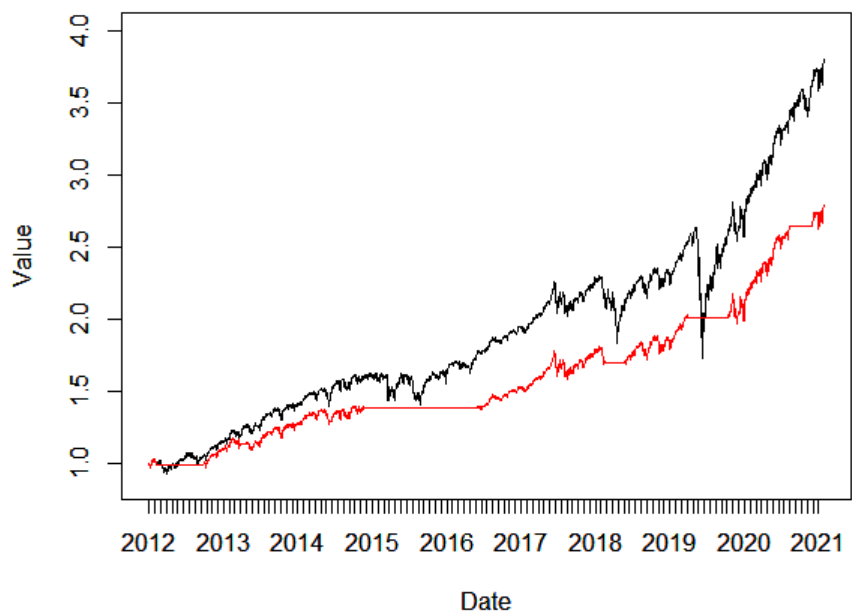


Fig. 7: 2012-2021: SP(black), Cash-(I14)-(C6)-(B1-4+&3-) (red)

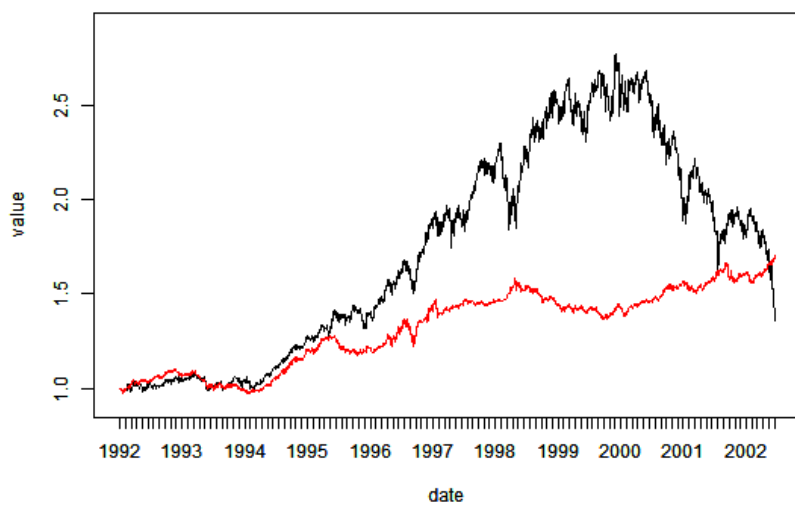


Fig. 8: 1992-2002: SP(black), TY-(I12)-(C6)-(B1-1+&5-) (red)

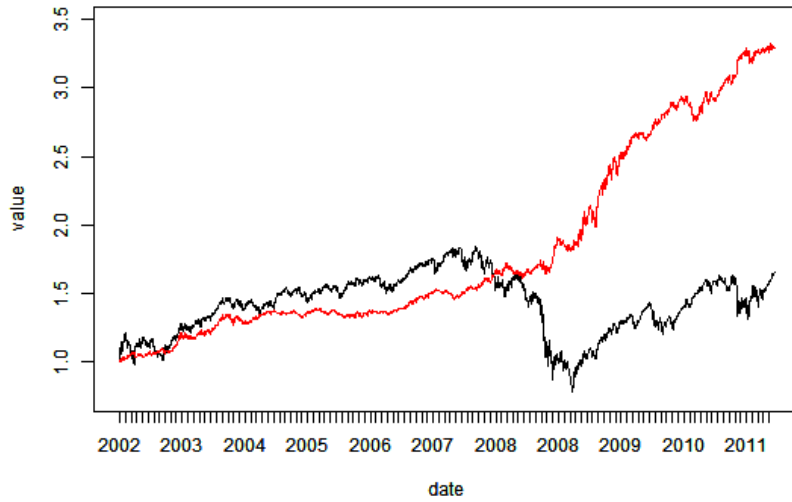


Fig. 9: 2002-2011: SP(black), TY-(I12)-(C6)-(B1-1+&5-) (red)

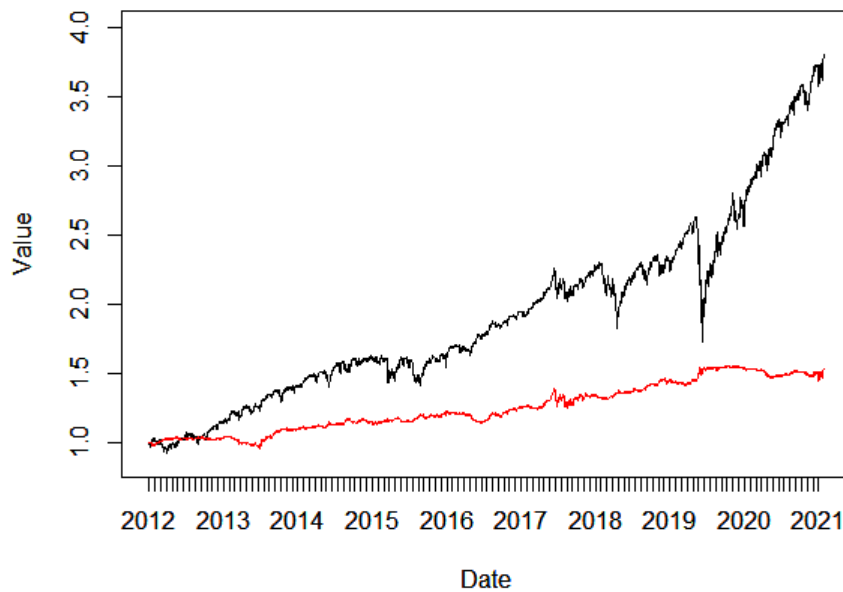


Fig. 10: 2012-2021: SP(black), TY-(I12)-(C6)-(B1-1+&5-) (red)

#### 4.4 An Extension to Constant Proportion Strategy

This section investigates an extension of the strategy in the previous Section 4.3 to constant proportion strategies. That is, in the previous section, SP long-only strategy is employed in

normal periods, while that SP position is shifted to the cash or TY under a specific condition expressed by the three attributes of the indicators (I1)-(I24), the investment conditions (C1)-(C6) and the boundary values (B1)-(B2) such as “(I12)-(C6)-(B1-1+&5-)”. On the contrary, this section tests the static 3:7 strategy of SP and TY,  $\omega_t \equiv (0.3, 0.7)$ , is adopted in normal periods, while the proportion is shifted to 1:9,  $\omega_t \equiv (0.1, 0.9)$ , under the same conditions used in the previous Section 4.3.

As a result of investment simulations, the case (I14)-(C6)-(B1-4+&3-), which also shows the best performance in the SP-Cash cases in Section 4.3, attains the highest Sharpe ratio in the current experiment. Here, we denote this case as Static-(I14)-(C6)-(B1-4+&3-). As shown in Table 6 and Fig. 11, the proposed model entirely improves the traditional static 1:9 and 3:7 strategies including returns, risk-adjusted returns and maximum drawdown.

Table 6: Performance Ratio: Static Strategies

	Static-(I14)-(C6)-(B1-4+&3-)	1:9 Strategy	3:7 Strategy
Average Return(per annum)	5.5%	4.0%	4.8%
Standard Deviation(per annum)	5.3%	5.1%	6.1%
Downside Deviation (per annum)	3.8%	3.6%	4.3%
Maximum Drawdown	10.7%	11.0%	13.1%
Sharpe ratio(per annum)	1.03	0.79	0.79
Sortino ratio(per annum)	1.46	1.12	1.13
Sterling ratio (per annum)	0.52	0.37	0.37

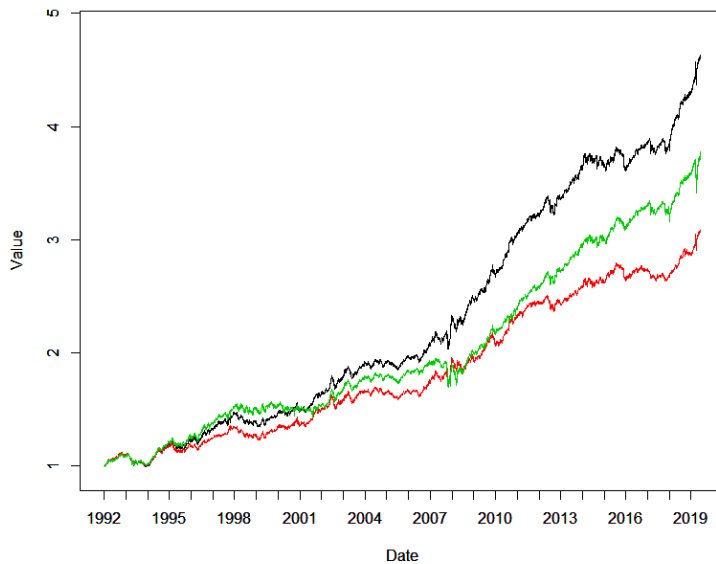


Fig. 11: Portfolio Value:  
Static-(I14)-(C6)-(B1-4+&3-) (black), 1:9 Strategy (red), 3:7 Strategy (green)

## 5 Conclusion

This research has presented a new state-space approach to explain financial market dynamics driven by trading activities of the three types of traders; trend follower, contrarian and yield curve-based equity traders. Particularly, based on the assumption that the price changes are represented by a linear combination of those different trades, PF-based state estimation has revealed the dynamic changes of the price impacts by those different types of trading. In other words, this paper has proposed a novel factor decomposition method on price changes from a perspective of the traders' demand/supply, which enables us to analyze the current market conditions and the possible risks in financial markets.

In the empirical studies with S&P 500 and US 10 year treasury note, after confirming the success of replicating the S&P 500 price, the new signals to detect signs of market crashes have been introduced based on the estimated states. Especially, it has been found that the demand of yield curve-based traders subtracting that of trend-followers could be a promising signal of stock market crashes, which has successfully enhanced the simple buy-and-hold strategy of S&P 500, as well as constant proportion strategies.

## Appendix: Algorithm of Particle filter

In this paper, we use the following PF algorithm developed by Gordon et al. (1993) and Kitagawa (1996). First of all, the Bayes formula shows

$$p(Z_t|O_{1:t}) \propto p(O_t|Z_t)p(Z_t|O_{1:t-1}). \quad (26)$$

Then, we apply a sampling importance resampling (SIR) method to obtain the samples  $\{\hat{Z}_t^{[\ell]}\}_{\ell=1,\dots,L}$  from the posterior  $p(Z_t|O_{1:t})$ . That is, by regarding the prior  $p(Z_t|O_{1:t-1})$  as an importance function, we first draw  $\{Z_t^{[\ell]}\}_{\ell=1,\dots,L}$  from the distribution  $p(Z_t|O_{1:t-1})$ , then resample from them with weights proportional to the likelihood  $p(O_t|Z_t)$ , which gives us  $\{\hat{Z}_t^{[\ell]}\}_{\ell=1,\dots,L}$ . These random samples are called "particles" in the PF literature.

Here, we get the samples  $\{Z_t^{[\ell]}\}_{\ell=1,\dots,L}$  from the prior  $p(Z_t|O_{1:t-1})$  in the following way. Note that

$$\begin{aligned} p(Z_t|O_{1:t-1}) &= \int \int p(Z_t, Z_{t-1}, v_t|O_{1:t-1})dZ_{t-1}dv_t \\ &= \int \int p(Z_t|Z_{t-1}, v_t)p(v_t)p(Z_{t-1}|O_{1:t-1})dZ_{t-1}dv_t \\ &= \int \int \delta(Z_t - G(Z_{t-1}, v_t))p(v_t)p(Z_{t-1}|O_{1:t-1})dZ_{t-1}dv_t, \end{aligned} \quad (27)$$

where  $\delta(\cdot)$  is the Dirac delta function. Then, for given the samples of  $\{v_t^{[\ell]}\}_{\ell=1,\dots,L}$  and  $\{\hat{Z}_{t-1}^{[\ell]}\}_{\ell=1,\dots,L}$  from  $p(v_t)$  and  $p(Z_{t-1}|O_{1:t-1})$ , respectively, we obtain the samples  $\{Z_t^{[\ell]}\}_{\ell=1,\dots,L}$  from  $p(Z_t|O_{1:t-1})$  by setting  $Z_t^{[\ell]} = G(\hat{Z}_{t-1}^{[\ell]}, v_t^{[\ell]})$ .

Thus, the PF algorithm is summarized as follows:

- (i) Generate the initial state vector  $\{\hat{Z}_0^{[1]}, \dots, \hat{Z}_0^{[L]}\}$ .
- (ii) Apply the following steps (ii-a)~(ii-d) to each time  $t = 1, \dots, T$ .
  - (ii-a) Generate system noise  $v_t^{[\ell]}$ ,  $\ell = 1, \dots, L$ .



- (ii-b) Compute for each  $\ell = 1, \dots, L$   
 $Z_t^{[\ell]} = G(\hat{Z}_{t-1}^{[\ell]}, v_t^{[\ell]}).$
- (ii-c) Evaluate the weights of particles  $\{Z_t^{[1]}, \dots, Z_t^{[L]}\}$  as  $\delta_t^{[\ell]} \equiv p(O_t | Z_t^{[\ell]})$ ,  $\ell = 1, \dots, L$  by using the likelihood function.
- (ii-d) Resample  $\{\hat{Z}_t^{[1]}, \dots, \hat{Z}_t^{[L]}\}$  from  $\{Z_t^{[1]}, \dots, Z_t^{[L]}\}$ . More precisely, resample each  $\hat{Z}_t^{[\ell]}$ ,  $\ell' = 1, \dots, L$  from  $\{Z_t^{[1]}, \dots, Z_t^{[L]}\}$  with the probability given by

$$\text{Prob.}(\hat{Z}_t^{[\ell]} = Z_t^{[\ell]} | O_t) = \frac{\delta_t^{[\ell]}}{\sum_{m=1}^L \delta_t^{[m]}}, \quad \ell = 1, \dots, L.$$

## Acknowledgment

The authors appreciate Mr. Souta Nakatani for his technical support.

## References

- [1] Alimoradi, M. R., & Kashan, A. H. (2018). A league championship algorithm equipped with network structure and backward Q-learning for extracting stock trading rules. *Applied Soft Computing*, 68, 478-493.
- [2] Arulampalam, M. S., Maskell, S., Gordon, N., & Clapp, T. (2002). A tutorial on particle filters for online nonlinear/non-Gaussian Bayesian tracking. *IEEE Transactions on signal processing*, 50(2), 174-188.
- [3] BlackRock (2018). What the yield curve can tell equity investors, Retrieved from <https://www.blackrock.com/americas-offshore/insights/what-the-yield-curve-can-tell-equity-investors/>. Accessed May29, 2020.
- [4] Cavalcante, R. C., Brasileiro, R. C., Souza, V. L., Nobrega, J. P., & Oliveira, A. L. (2016). Computational intelligence and financial markets: A survey and future directions. *Expert Systems with Applications*, 55, 194-211.
- [5] Chang, Y. H., & Lee, M. S. (2017). Incorporating Markov decision process on genetic algorithms to formulate trading strategies for stock markets. *Applied Soft Computing*, 52, 1143-1153.
- [6] L. Cocco, R. Tonelli, and M. Marchesi (2019). An agent-based artificial market model for studying the bitcoin trading. *IEEE Access*, 7:42908?42920.
- [7] Dash, R., Samal, S., Dash, R., & Rautray, R. (2019). An integrated TOPSIS crow search based classifier ensemble: In application to stock index price movement prediction. *Applied Soft Computing*, 85, 105784.
- [8] Fileccia, G., & Sgarra, C. (2018). A particle filtering approach to oil futures price calibration and forecasting. *Journal of Commodity Markets*, 9, 21-34.
- [9] Gordon, N., Salmond, D., & Smith, A. (1993). Radar and signal processing. In *IEEE Proceedings* (Vol. 140, pp. 107-113).

- [10] Kitagawa, G. (1996). Monte Carlo filter and smoother for non-Gaussian nonlinear state space models. *Journal of computational and graphical statistics*, 5(1), 1-25.
- [11] Kristjanpoller, W., & Michell, K. (2018). A stock market risk forecasting model through integration of switching regime, ANFIS and GARCH techniques. *Applied Soft Computing*, 67, 106-116.
- [12] Lei, L. (2018). Wavelet neural network prediction method of stock price trend based on rough set attribute reduction. *Applied Soft Computing*, 62, 923-932.
- [13] Liu, H., & Sun, F. (2012). Efficient visual tracking using particle filter with incremental likelihood calculation. *Information Sciences*, 195, 141-153.
- [14] Long, J., Chen, Z., He, W., Wu, T., & Ren, J. (2020). An integrated framework of deep learning and knowledge graph for prediction of stock price trend: An application in Chinese stock exchange market. *Applied Soft Computing*, 106205.
- [15] Mamdani, E. H., & Assilian, S. (1975). An experiment in linguistic synthesis with a fuzzy logic controller. *International journal of man-machine studies*, 7(1), 1-13.
- [16] Nakatani, S., Nishimura, K. G., Saito, T., & Takahashi, A. (2020). Interest rate model with investor attitude and text mining. *IEEE Access*, 8, 86870-86885.
- [17] Nakano, M., Takahashi, A., & Takahashi, S. (2017). Generalized exponential moving average (EMA) model with particle filtering and anomaly detection. *Expert Systems with Applications*, 73, 187-200.
- [18] Nakano, M., Takahashi, A., & Takahashi, S. (2017). Creating investment scheme with state space modeling. *Expert Systems with Applications*, 81, 53-66.
- [19] Nakano, M., Takahashi, A., & Takahashi, S. (2017). Fuzzy logic-based portfolio selection with particle filtering and anomaly detection. *Knowledge-Based Systems*, 131, 113-124.
- [20] Nakano, M., Takahashi, A., & Takahashi, S. (2017). Robust technical trading with fuzzy knowledge-based systems. In *SoMeT*, pages 652-667.
- [21] Nakano, M., Takahashi, A., Takahashi, S., & Tokioka, T. (2018). On the effect of Bank of Japan's outright purchase on the JGB yield curve. *Asia-Pacific Financial Markets*, 25(1), 47-70.
- [22] Nakano, M., & Takahashi, A. (2020). A new investment method with AutoEncoder: Applications to crypto currencies. *Expert Systems with Applications*, 162, 113730.
- [23] Orchard, M. E., & Vachtsevanos, G. J. (2009). A particle-filtering approach for on-line fault diagnosis and failure prognosis. *Transactions of the Institute of Measurement and Control*, 31(3-4), 221-246.
- [24] Ramezani, R., Peymanfar, A., & Ebrahimi, S. B. (2019). An integrated framework of genetic network programming and multi-layer perceptron neural network for prediction of daily stock return: An application in Tehran stock exchange market. *Applied soft computing*, 82, 105551.
- [25] Sugeno, M., & Kang, G. T. (1988). Structure identification of fuzzy model. *Fuzzy sets and systems*, 28(1), 15-33.

- [26] Takagi, T., & Sugeno, M. (1985). Fuzzy identification of systems and its applications to modeling and control. *IEEE transactions on systems, man, and cybernetics*, (1), 116-132.
- [27] Takahashi, A., & Takahashi, S. (2021). A new interval type-2 fuzzy logic system under dynamic environment: Application to financial investment. *Engineering Applications of Artificial Intelligence*, 100, 104154.
- [28] Tang, H., Dong, P., & Shi, Y. (2019). A new approach of integrating piecewise linear representation and weighted support vector machine for forecasting stock turning points. *Applied Soft Computing*, 78, 685-696.
- [29] Yang, F., Chen, Z., Li, J., & Tang, L. (2019). A novel hybrid stock selection method with stock prediction. *Applied Soft Computing*, 80, 820-831.
- [30] Zadeh, L.A. (1965). Fuzzy sets. *Information and control*, 8(3):338-353.
- [31] Zadeh, L.A. (1999). Fuzzy sets as a basis for a theory of possibility. *Fuzzy sets and systems*, 100:9-34.
- [32] Zhou, F., Zhang, Q., Sornette, D., & Jiang, L. (2019). Cascading logistic regression onto gradient boosted decision trees for forecasting and trading stock indices. *Applied Soft Computing*, 84, 105747.